Apparatus for measuring viscoelastic properties over ten decades: refinements

Review of Scientific Instruments, 66(11), 5292-5297 (1995).

M. Brodt, L. S. Cook and R. S. Lakes§

§ Department of Engineering Physics
Engineering Mechanics Program; Biomedical Engineering Department
Materials Science Program and Rheology Research Center
University of Wisconsin-Madison
147 Engineering Research Building
1500 Engineering Drive, Madison, WI 53706-1687
Office phone (608) 265-8697; fax: (608) 263-7451

Address correspondence to R. S. Lakes

Abstract

This article describes refinements to an instrument for determining the viscoelastic properties of a solid material isothermally, with a single apparatus, over 10 decades of time and frequency. Torque is applied electromagnetically to a specimen fixed at one end. Specimen deformation is determined via a laser beam reflected from the other end upon a split diode detector. Phase resolution is improved by the use of a lock in amplifier at high frequency and by the use of Lissajous figures to measure phase, allowing study of materials of moderate loss ($0.008 \leq \tan\delta \leq 0.2$) in addition to materials with high loss ($\tan\delta \approx 1$). The rigidity of the instrument is increased by modifications in the specimen support geometry. The range of equivalent frequency for torsion is from less than 10^{-6} Hz to more than 10^{4} Hz. Digital methods are incorporated in the creep measurements and in phase measurements.

I. INTRODUCTION

In a previous paper from this laboratory [1] , Chen and Lakes reported the development of an instrument for mechanical characterization of viscoelastic materials over a wide range of ten decades (a factor of 10^{10}) of time and frequency. It was capable of quasi-static, subresonant dynamic, and resonant experiments in torsion and in bending. The mechanical portion of the instrument is shown schematically on the left of Fig. 1.

The rationale for the development of such an instrument is as follows. A variety of instruments and methods are available for viscoelastic studies as reviewed by Ferry [2]. Most such methods cover a few decades or less of time or frequency. For example, the Fitzgerald apparatus [3] applies a shear load to solids or liquids and permits the operator to infer mechanical properties from measurements of electrical impedance. The frequency range covers 1.7 decades from 100 Hz to 5 kHz [3]. Static experiments cannot be done with this apparatus. The multiple lumped resonator concept of Birnboim has been applied by Schrag and Johnson [4] to viscoelastic measurements on fluids. In this approach, torsional oscillations are set up in a system of cylindrical inertia members joined by rods. Angular displacement is measured by reflecting light from a mirror on the oscillator and modulating the light intensity via Ronchi gratings. This is a resonant method which provides data at discrete frequencies from 100 Hz to 8300 Hz: two decades. Quasistatic experiments cannot be done with this apparatus, however modifications of the Birnboim apparatus permit low frequency studies down to 0.01 Hz [5]. Recent developments in signal processing permit good precision down to 10^{-6} Hz [6]. High frequency studies may be conducted using resonance or wave propagation methods as reviewed by McSkimin [7]. For example, the piezoelectric composite oscillator method makes use of quartz crystals to excite a solid specimen [8,9] ultrasonically in longitudinal or torsional resonance or a fluid [10] in shear. Such methods do not allow quasistatic or low frequency measurements, however by exciting higher harmonics in the quartz rod, it is possible to obtain more than one decade. An automated creep apparatus described by Plazek [11] makes use of electromagnetic drive and optical measurement of rotation. It covers a range of time from about half a second to several days: six decades.

For some materials, particularly amorphous polymers, it is possible to infer material properties over a wider range from test results taken at different temperatures. Materials for which such a procedure is possible are called thermorheologically simple. Many examples covering 12 or more decades are known [2,11]. Many materials, particularly composites and materials in which multiple viscoelastic mechanisms are active, are not thermorheologically simple. Direct measurement of properties over many decades is required for a full characterization of the material. In most experiments which isothermally cover a wide range of frequency, a set of different experiments is performed, each one conducted with a different instrument [12]. A range of 6.5 decades was attained with two devices, one for 0.0002 Hz to 30 Hz, and a second device for 20 to 1000 Hz [13], a range of 6 decades (10^{-5} to 10 Hz) with one device [14] and a range of 8 decades [15] (10^{-6} to 100 Hz) with one device. In such instruments, the low frequency limit is dictated primarily by the experimenter's patience in conducting lengthy dynamic or creep tests, and secondarily by mechanical drift or by drift in any electronics used. If one is willing to perform creep tests lasting several years, with a rise time less than one second, it is possible to achieve many decades [16]. The upper frequency limit is governed by resonances in the specimen and in the instrument and how they are dealt with.

In the prior version of the present instrument, the specimen was attached, using a cyanoacrylate adhesive, to a vertical rod connected to a rigid framework of rods. A disc shaped permanent magnet, made of high intensity neodymium-iron-boron, and a small mirror were attached, using the same adhesive, to the free end of the specimen. A current was applied to the Helmholtz coil, thus loading the specimen through the action of the coil's magnetic field on the magnetic driving disc. Angular displacement was measured by laser interferometry. An image of the first grating was formed on the specimen's mirror and projected through the second grating. The interaction of the moving image of the first grating and the fixed second grating resulted in interference fringes proportional to angular displacement. The fringe signal was converted to an electronic signal by the light detector.

For the case of a quasi-static test (creep), the input to the Helmholtz coil was a DC signal which resulted in a constant torque at the end of the specimen. Angular displacement was measured as a function of time t and the creep compliance, J(t), was calculated as the ratio of creep strain to applied stress. For the case of a dynamic experiment, the input to the Helmholtz coil was an AC signal which resulted in a sinusoidal torque of known magnitude at the end of the specimen. Angular displacement was measured. The absolute dynamic modulus $|M(\omega)|$ and the loss tangent, $\tan\delta$, were inferred via an inversion of the exact analytical solution of the problem of dynamic torsion of a rod fixed at one end and with a mass at the other end. This analysis is valid both for resonant conditions and through resonances, for $\tan\delta$ of any magnitude. This approach was particularly useful for viscoelastic elastomers with a high $\tan\delta$. For low-loss materials it was also possible to calculate $\tan\delta$ from the width of the frequency response curve, as is commonly done.

The wide range of time and frequency (ten decades) was achieved by minimizing the inertia attached to the specimen, using a simple specimen geometry governed by a known analytical solution amenable to numerical inversion, and using driving and detection methods free of resonances and also capable of quasi-static tests.

The instrument proved very useful for mechanical characterization of low-stiffness, high-loss materials such as polymers and viscoelastic elastomers. Its limitations became apparent recently when the laboratory began investigating candidate materials for use as constituents in high-stiffness, high-loss metal-matrix composites. Specifically, instrument compliance affected experimental results for some thick specimens and phase resolution was found to be insufficient for materials of $\tan\delta$ less than 0.1. This paper reports a series of refinements to the instrument described in Ref. 1: instrument stiffness has been increased to allow testing of specimens with greater rigidity; phase resolution has been increased to provide higher precision in subresonant tests; and digital data acquisition has been incorporated.

II. THEORY

Ideally, in order to characterize the constitutive behavior of a material, one applies the input variable and observes the response of the output variable. However stress is not readily observable; one measures force or torque. The relationship between stress and torque and between strain and angular displacement is provided by the solution of a boundary value problem for the specimen geometry in question. For dynamic torsional experiments, an exact solution exists for the boundary value problem for a solid rod of circular cross section. For the case of bending, quasi-static experiments can be analyzed approximately using the corresponding exact analytical solution for static bending. At resonances, damping can be calculated using the method of resonant half-widths. The remainder of the paper will be

concerned with the torsion experiment, with the understanding that bending experiments can be performed in a similar manner.

A. Creep Experiments.

Creep experiments were conducted by using a step function input to the bipolar amplifier which drives the coil, to apply a torque constant in time, to the free end of the specimen. Shear stress, τ, is calculated from the torque and specimen geometry. Shear strain, γ, is calculated from the angular displacement and specimen geometry. Creep compliance was calculated from the measured torque M, angular displacement φ, and specimen rod radius r and length L using the quasistatic relation

$$J(t) = \frac{\varphi(t)\frac{\pi r^4}{2}}{ML} \qquad (1)$$

B. Dynamic Experiments.

At frequencies significantly below that of the specimen's first torsional resonance, the stiffness considered as the absolute value of the complex shear modulus G^* has an approximate value given by the quasistatic relation

$$|G^*| = \left|\frac{ML}{\varphi\frac{\pi r^4}{2}}\right|. \qquad (2)$$

Due to dynamic effects, the apparent stiffness changes by 5% at 0.22 of the lowest resonance frequency, however all results were analyzed dynamically, via Eq. (4).

Damping, the phase δ between stress and strain, in the quasistatic domain (at frequencies well below any resonance) is approximately equal to the measured phase φ between torque and angular displacement:

$$\tan\delta \approx \tan\varphi \qquad (3)$$

The phase φ differs from δ by 10% at 0.3 of the lowest resonance frequency; again, results were analyzed dynamically, via Eq. (4).

At frequencies approaching and including the specimen's first torsional resonance, the effect of specimen inertia and magnet inertia becomes important. Stiffness and damping were calculated by numerical solution of an exact relationship for the torsional rigidity (ratio of torque M* to angular displacement Φ) of a viscoelastic cylinder of radius R length L, and density ρ with an attached mass of mass moment of inertia I_{at} at one end and fixed at the other end [13]:

$$\frac{M^*}{\Phi} = [\pi\rho\pi R^4][\omega^2 L]\frac{\cot\Omega^*}{\Omega^*} - I_{at}\omega^2 \ , \qquad (4)$$

where $\Omega^* = \sqrt{\frac{\rho\omega^2 L^2}{KG^*}}$, K is a geometrical constant (equal to 1 for a cylindrical specimen with circular cross section). Calculations were performed using this exact formulation except for specimens of moderate to low loss studied via free decay or resonance half width, as discussed below. Inversion of Eq. 4 was carried out via a numerical procedure based on Newton's method [1]. Coupling with flexural modes has not been a problem. Such coupling would manifest itself as a spurious resonance at intermediate frequencies below the first torsional mode. Such effects were minimized by making the specimen and the end attachment as symmetrical as possible.

For materials of comparatively low loss at frequencies corresponding to a resonant torsional or bending resonant mode of the specimen, damping was calculated using the shape of the frequency response curve near the resonance (the resonance half-width method):

$$\tan\delta \approx \frac{1}{\sqrt{3}}\frac{\Delta\omega}{\omega_0}, \qquad (5)$$

where $\Delta\omega$ is the full width of the resonance curve at half maximum. A related approach using the width at $1/\sqrt{2}$ of maximum is valid within 1% for $\tan\delta \leq 0.28$ [17].

At the higher frequencies some energy is transmitted into the support rod, giving rise to a parasitic loss. The amount of transmitted energy can be evaluated via the mechanical impedance Z. For longitudinal waves, Z is the ratio of driving force to particle velocity [7]; for a rod of radius r, density ρ, and complex Young's modulus E*, Z depends on the cross sectional area.

$Z = \pi r^2 \sqrt{\rho E^*}$.

The impedance for torsion is the ratio of torque to angular velocity; it depends on the polar moment of inertia.

$Z = ¤\pi r^4 \sqrt{\rho G^*}$. (6)

This is in contrast to the case of plane shear waves in which there is no mismatch in area or moment of inertia:

$Z = \sqrt{\rho G^*}$ represents the characteristic impedance.

The reflection coefficient, defined as the ratio of stress in the reflected wave to the stress in the incident wave, is [18]

$$R = \frac{Z_1 - Z_2}{Z_1 + Z_2} . \quad (7)$$

The transmission coefficient for power is [18]

$$T_p = 1 - |R|^2 = \frac{4}{\left[\sqrt{\frac{Z_2}{Z_1}} + \sqrt{\frac{Z_1}{Z_2}}\right]^2} . \quad (8)$$

The difference in diameter between the specimen and the support rod gives rise to an impedance mismatch which parasitic loss resulting from transmission of waves into the support. Since in torsion the impedance goes as the fourth power of diameter, the desired impedance mismatch can be large. As an example, consider medium 2, the support rod, to be steel, with G = 78 GPa, ρ = 7.9 g/cm^3, r = 6.2 mm, and material 1, a specimen, to be aluminum alloy with G = 27 GPa, ρ = 2.7 g/cm^3, r = 0.8 mm. Then $T_p = 4.7 \times 10^{-3}$; considering this as a parasitic specific damping or energy ratio Ψ_p, the parasitic loss tangent is

$\tan\delta_p = \frac{1}{2\pi}\Psi_p = 0.75 \times 10^{-3}$.

Most of the materials studied have been considerably more compliant than aluminum hence would present less problem of parasitic loss. Moreover use of a tungsten support rod (E = 400 GPa, ρ = 19.3 g/cm^3, r = 6.2 mm) further reduces parasitic loss when studying stiff specimens. For measurements of materials of extremely small damping, a free-free resonance method is recommended, however such methods are not amenable to static measurements.

III. PROCEDURES

Determination of angular displacement and of torque

Light from the laser was reflected from the specimen's mirror to a split-diode silicon light detector (Centronics Co.). The optical lever approach to measuring angular displacement is time-honored, effective, and used in a variety of instruments [19]. Use of a laser in the present instrument allows a small mirror of small inertia to be used. The detector was connected to a differentialpreamplifier built into a small circuit box, shown in Fig. 2. The rationale for this arrangement was to avoid cable capacitance which would introduce unacceptably large phase errors. The detector-preamplifier assembly was mounted on a small micrometer driven stage which was used for *in situ* calibration of the detector system. Calibration was achieved by preparing a plot of output voltage versus micrometer displacement. A correction curve for amplifier phase shifts at high frequency was obtained by measuring the phase between torque and angular displacement of a rod of aluminum alloy with known small loss tangent (type 6061-T6, E = 68.9 GPa, G = 25.9 GPa, $\tan\delta \approx 3.6 \times 10^{-6}$) [20]. The detector provides a linear voltage response to angular displacement, in contrast to the interferometric approach used earlier in which the output voltage signal V was $V = A \sin k\Phi + B$ in which Φ is the angular displacement. Use of a linear detection scheme centered about zero permits a variety of methods to be used for phase

determination, as described below. Typical angular displacement was less than 1 mrad, and surface shear strain less than 10^{-5}. An increased displacement range for creep can be obtained if the laser beam is intentionally off center within the linear range at the start of the experiment.

Torque was inferred from the current in the coil as determined from the voltage across a non-inductive series resistor. Calibration of this relationship was achieved by testing of a standard specimen of 6061 aluminum alloy, which has been very well characterized. An absolute calibration procedure was used earlier [1] however it is more cumbersome.

Phase measurement

Procedures were developed to improve the phase resolution of the instrument. In the previous version of the instrument, the phase difference between the torque and angular displacement signals was taken from the time delay between the signals as observed on an oscilloscope. This approach provided sufficient phase resolution to study high loss viscoelastic elastomers. To improve measurement aspects of phase resolution in the present version, a lock-in amplifier (Ithaco, 2961B) is used for frequencies between 1 to 10 Hz and 10 kHz. The phase resolution is 0.01°, or 1.8×10^{-4} rad. The lock in amplifier has a lower frequency limit of 0.5 Hz, and its performance begins to suffer as that limit is approached. At lower frequencies, a Lissajous figure was examined on a digital oscilloscope or on a computer (Macintosh IIci with Labview hardware and software) to determine phase. The input channels are 12 bits, so for a full scale signal, the digital limit on phase resolution is $[4096]^{-1} = 2.4 \times 10^{-4}$ rad. Phase determination by the method of Lissajous figures can provide high resolution if the figure is expanded; the method is particularly useful at low frequency [21]. Improvements in mechanical aspects of phase resolution were achieved by reducing mechanical perturbations. Noise from building vibration was reduced by a change of environment and by use of additional foam isolation beneath the instrument. Low frequency noise from air currents was reduced by a baffle around the instrument. The actual phase resolution in the Lissajous figures was about 0.001 rad; it is limited by residual mechanical perturbations. The phase φ was extracted from the maximum width A of the elliptic load-deformation plot of a linearly viscoelastic material by $\sin \varphi = A/B$ with B as the peak-to peak signal level. Use of Lissajous figures was facilitated by the modified detection scheme which eliminated the DC offset which was present in the single-element detector used in the interferometric approach. At specimen resonances in materials with moderate loss, the method of resonant half-width was used, as in the previous instrument; this method is very accurate.

Dominant error sources in specimens with moderate damping differ from those which are important in the high loss materials ($\tan \delta \approx 1$) discussed earlier [1]. For high loss materials, the method of resonance half width cannot be used since the approximate formula fails for such broad resonances; numerical inversion of the resonance was conducted. The specimen diameter and density must be known accurately to calculate large $\tan \delta$ by the inversion approach. For materials with low to moderate loss ($\tan \delta \leq 0.1$), analysis is simpler since the method of resonance half width can be used near resonance; moreover that method is insensitive to any uncertainty in specimen diameter or density. Below resonance, the correction for inertial terms is less sensitive to specimen geometry than in the case of high loss materials.

Frequency range

Above about 2 kHz it became difficult to pass sufficient current through the Helmholtz coil as a result of its inductive reactance. This reactance was neutralized with the aid of switched capacitors placed in series with the coil, with additional capacitors provided for several frequency ranges up to 14 kHz. It became possible to excite higher harmonics in the torsional resonance spectrum by this approach. The capacitors did not introduce phase error since the drive current is determined from the voltage across a resistor, not from the voltage across the coil. In measurements involving higher harmonics, the method of free-decay of vibration was also used.

Instrument stiffness

It was considered desirable to increase the rigidity of the instrument in order to accommodate larger diameter specimens which are examined on occasion. For that purpose, the rod which supports the specimen was changed from an aluminum rod (E = 70 GPa) to a tungsten one (E = 400 GPa). Rods were 12.7 mm in diameter; the support rod was 310 mm in length, and the portion protruding beyond the fixture depended on the specimen length; typically 160 mm. For most slender specimens, a stainless steel support rod was sufficient. Moreover the clamp supporting the specimen rod was replaced with a large

steel block in which holes were drilled to accept the connecting rods, which were changed from aluminum to stainless steel. Instrument stiffness was determined with the aid of a large magnet cemented directly to the support rod to generate torque.

Digital processing

Data were acquired using Labview® software and associated electronics (a multifunction I/O board and a GPIB instrument controller; National Instruments Inc.) in conjunction with a Macintosh® IIci computer. The input channels have 12 bit resolution. Creep data were obtained in the form of a specified number of data points per logarithmic decade. Data were stored in a file for later export into routines for analysis and graphical presentation. Both the torque and angular displacement signals were recorded as functions of time. As for dynamic tests, the recording and interpretation of Lissajous figures was facilitated by storing the data digitally, and displaying a plot of torque vs angular displacement on the computer. This approach was particularly helpful at low frequencies (below 0.1 Hz) for which the use of an oscilloscope becomes tedious. The capability for averaging was also incorporated, to reduce the effect of low frequency noise. Cursors providing a read-out of input and output voltage were incorporated to aid the experimenter in extracting data in digital form from the Lissajous figure.

IV. RESULTS

The final instrument stiffness was about 3×10^6 N-mm/rad. This is orders of magnitude greater than the stiffness of the specimens examined, which were typically 3 mm in diameter, in comparison with the 12.7 mm diameter support rod. Instrument stiffness therefore contributed negligible error to the measured stiffness of such specimens. The dominant source of error in specimen stiffness is the measurement of the specimen diameter, since its structural rigidity is proportional to the fourth power of the diameter. Such errors are not associated with the instrument itself.

An experimental evaluation of parasitic loss was performed by measuring the damping of a low-loss material. A specimen of type 6061-T6 aluminum alloy, 1.5 mm in diameter, was examined. This specimen was cemented to a steel support rod. The tan δ obtained at resonance (1190 Hz) by the method of resonant half-width, was 7.8×10^{-4}. The value of tan δ obtained by a free-free resonant procedure [20] was 3.6×10^{-6}. The value 7.8×10^{-4} is in reasonable agreement with the parasitic loss calculated from mechanical impedance above. Since most materials tested were more compliant than aluminum, this value may therefore be considered an upper bound on the spurious loss due to transmission of energy into the support. This parasitic loss is much smaller than the smallest damping actually measured with the apparatus. A tungsten support rod is available to provide additional mechanical impedance mismatch in order to reduce parasitic loss when studying stiff specimens. Therefore the above aluminum-steel example may be considered a worst-case scenario for parasitic damping.

A viscoelastic damping spectrum for a cast eutectic indium-tin alloy at 25.9 ± 0.3°C is shown in Fig. 3. Surface shear strain was 1.6×10^{-5} or less at 100 Hz. This material was chosen for illustrative purposes since it exhibits a substantial range of tan δ over the frequency range studied, and tan δ ν^n with n as a constant is expected over a substantial range of frequency. Error estimates for tan δ at the higher sub-resonant frequencies were comparable to or less than the size of the data points. Combined creep and dynamic results cover about 10.4 decades of effective time and frequency. The creep compliance followed a power law in time over the range examined, $J(t)$ t^n, with $n = 0.269$. For a power law transient response, the loss angle is $\delta = ¤n\pi$, so that for the very low frequency regime in indium-tin, the loss inferred from creep is tan $\delta = 0.42$, a figure which compares favorably with the results of direct measurements of tan δ at low frequency. As for the dynamic behavior, the two lowest resonances were observed with sufficient amplitude to infer damping. There are an unlimited number of higher resonances, but they occur at progressively smaller amplitudes (as $1/\nu^2$ if the end mass is negligible; faster otherwise), which limits the signal to noise ratio hence the attainable precision.

There are no standard materials for viscoelasticity studies, since the physical processes which give rise to viscoelastic behavior tend to depend on specimen preparation methods as well as on environmental variables such as temperature and humidity. Therefore detailed quantitative comparisons with other results cannot be made. Nevertheless study of a low-loss aluminum alloy as a limiting case indicates parasitic loss to be sufficiently small to permit study of slender specimens of materials of moderate loss ($0.008 \leq \tan \delta \leq 0.2$) as well as high loss ($\tan \delta \approx 1$).

Acknowledgment

We thank the ONR for their support of this work. We thank K. Goodwin for his efforts in programming the computer and Dean Macken for machining of parts.

References

1 C. P. Chen, and R. S. Lakes, "Apparatus for determining the viscoelastic properties of materials over ten decades of frequency and time," Journal of Rheology, **33**, 1231-1249 (1989).

2 J. D. Ferry, *Viscoelastic Properties of Polymers*, 2nd ed., (J. Wiley, NY, 1970).

3 E. R. Fitzgerald, "Mechanical resonance dispersion in metals at audio frequencies", Phys. Rev. **108**, 690-706, (1957).

4 J. L. Schrag and R. M. Johnson, "Application of the Birnboim multiple lumped resonator principle to viscoelastic measurements of dilute macromolecular solutions", *Rev. Sci. Instr.* **42**: 224-232 (1971).

5 J. L. Schrag and Ferry, J. D., "Mechanical techniques for studying viscoelastic relaxation processes in polymer solutions", *Faraday Symposia of the Chemical Society* **6**: 182-193 (1972).

6 G. Winther, D. M. Parsons, and J. L. Schrag, "A high-speed, high precision data acquisition and processing system for experiments producing steady state periodic signals", *J. Polymer Science, Part B: Polymer Physics*, **32**, 659-670, (1994).

7 H. J. McSkimin, "Ultrasonic methods for measuring the mechanical properties of liquids and solids", in Physical Acoustics, ed. E. P. Mason, Vol. **1A**, 271-334, (1964).

8 Marx, J., "Use of the piezoelectric gauge for internal friction measurements", Rev. Sci. Instr., **22**, 503-509, (1951).

9 Robinson, W. H., Carpenter, S. H., and Tallon, J. L., "Piezoelectric method of determining torsional mechanical damping between 40 and 120 kHz", J. Appl. Phys. **45**, 1975-1981, (1974).

10 Stokich, T. M., Radtke, D. R., White, C. C., and Schrag, J. L., "An instrument for precise measurement of viscoelastic properties of low viscosity dilute macromolecular solutions at frequencies from 20 to 500 kHz", J. Rheology, **38**, 1195-1210, (1994).

11 D. J. Plazek, "Magnetic bearing torsional creep apparatus", J. Polymer Science, part A-2, **6**, 621-638 (1968).

12 V. J. Koppellmann, "Uber die Bestimmung des dynamischen Elasticitatsmoduls und des dynamischen Schubmoduls im Frequenzbereich 10^{-5} bis 10^{-1} Hz", Rheologica Acta **1**: 20-28 (1958).

13 W. G. Gottenberg, and R. M. Christensen, "An Experiment for Determination of the Mechanical Property in Shear for a Linear, Isotropic Viscoelastic Solid," International Journal of Engineering Science, **2**, 45-56 (1964).

14 J. Woirgard, Y. Sarrazin , and H. Chaumet, "Apparatus for the measurement of internal friction as a function of frequency between 10^{-5} and 10 Hz," Review of Scientific Instruments, **48**, 1322-1325 (1977).

15 R.S. Lakes, J.L. Katz, and S.S. Sternstein, "Viscoelastic properties of wet cortical bone: Part I, torsional and biaxial studies." Journal of Biomechanics, **12**, 657-678, (1979).

16 W. Letherisch, "The rheological properties of dielectric polymers", British J. Appl. Physics, **1**, 294-301, 1950.

17 E. J. Graesser, and C. R. Wong, "The relationship of traditional damping measures for materials with high damping capacity: a review", in M^3D: *Mechanics and Mechanisms of Material Damping*, Ed. V. K. Kinra, A. Wolfenden, (ASTM ,1916 Race St. Phila. PA, 1992).

18 L. Cremer, and M. Heckl, *Structure Borne Sound*, 2nd ed., (Springer Verlag, Berlin, 1986).

19 R. V. Jones, "Some developments and applications of the optical lever", *J. Sci. Instr.* **38**: 37-45 (1961).

20 W. Duffy, "Acoustic quality factor of aluminum alloys from 50 mK to 300 K", J. Appl. Phys. **68**, 5601-5609, (1990).

21 B. J. Brennan , "Linear viscoelastic behaviour in rocks", in *Anelasticity in the Earth*, ed. F. D. Stacey, M. S. Paterson, A. Nicholas, (Am. Geophysical Union, 1981).

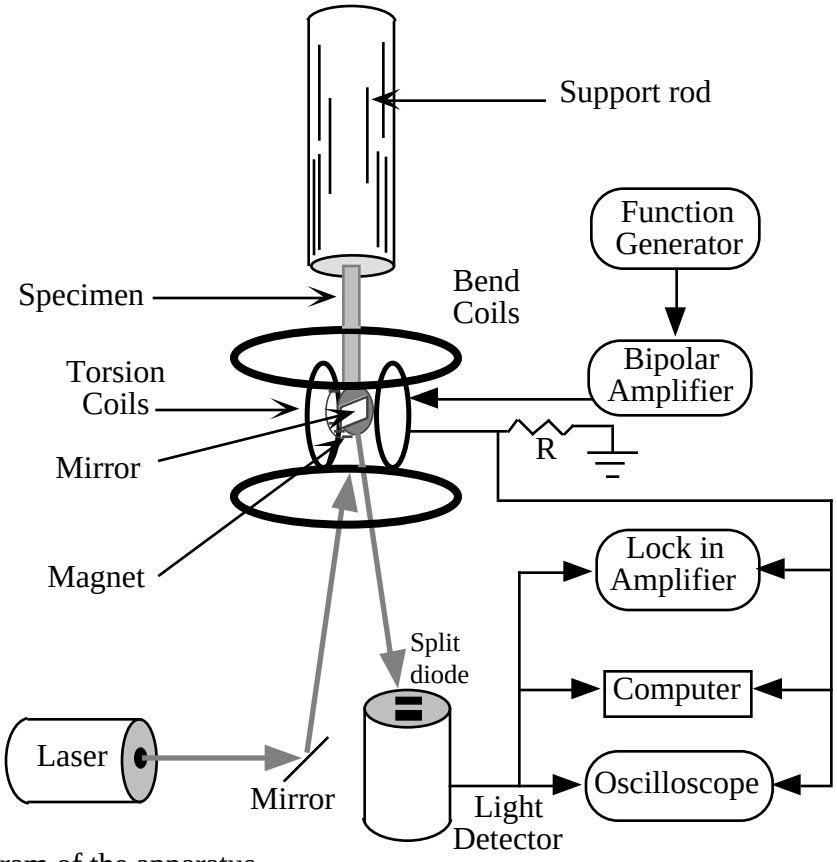

1 Schematic diagram of the apparatus.

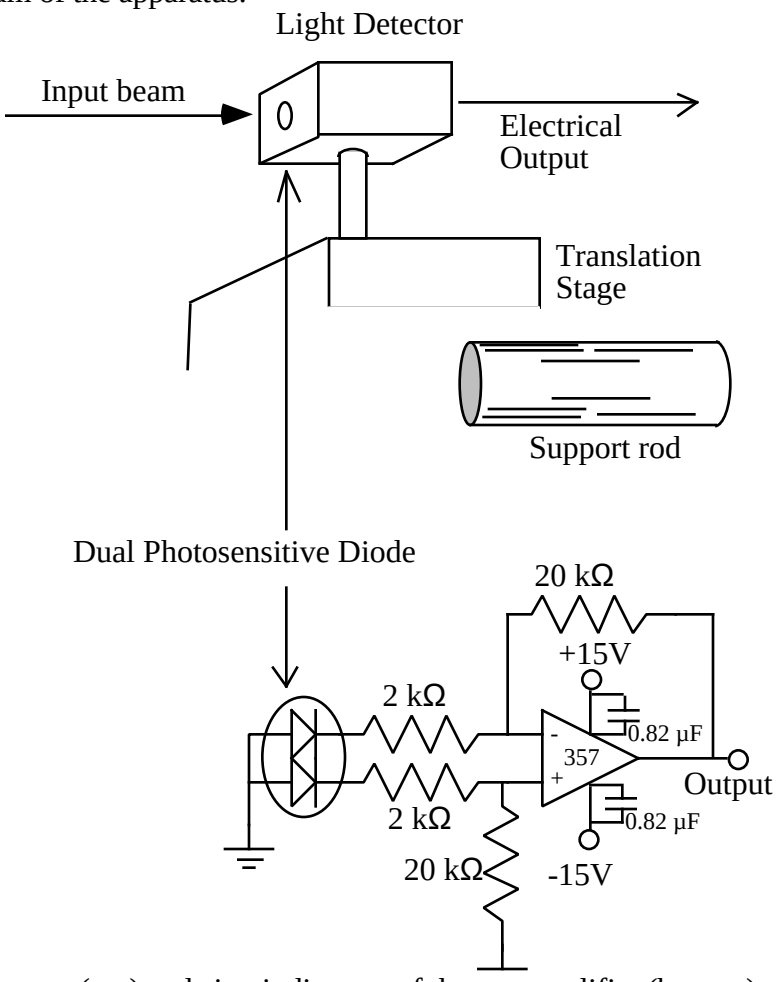

2 Detail of light detector (top) and circuit diagram of the pre-amplifier (bottom).

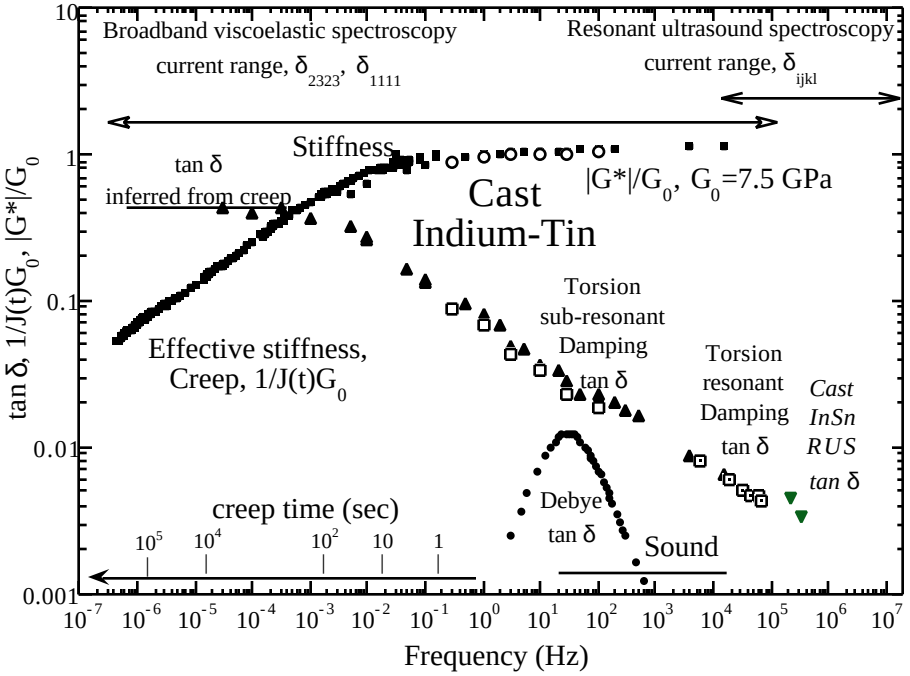

3 Viscoelastic behavior of indium-tin eutectic alloy at room temperature. Creep as a function of time t and dynamic results as a function of frequency ν shown on the same plot using the relation $2\pi\nu = t$. Circles: effective stiffness. Triangles: tan δ. Open triangles, sub-resonant; solid triangles, resonant, first two modes. G_o is a normalizing stiffness, taken at 100 Hz.

For comparison, a Debye peak based on a three-element viscoelastic model and preliminary results from resonant ultrasound spectroscopy are also shown.